prb 77 2008 104439

Dataset · March 2014

10 authors, including:

Nikolai A. Sobolev
University of Aveiro
151 PUBLICATIONS **957** CITATIONS
SEE PROFILE

Manuel Valente
University of Aveiro
51 PUBLICATIONS **319** CITATIONS
SEE PROFILE

Katsuaki Sato
Tokyo University of Agriculture and Technology
269 PUBLICATIONS **2,755** CITATIONS
SEE PROFILE

Sergio Gama
Universidade Federal de São Paulo
163 PUBLICATIONS **1,975** CITATIONS
SEE PROFILE

Influence of the strong magnetocrystalline anisotropy on the magnetocaloric properties of MnP single crystal

M. S. Reis*
CICECO, Universidade de Aveiro, 3810-193 Aveiro, Portugal

R. M. Rubinger
Departamento de Física and I3N, Universidade de Aveiro, 3810-193 Aveiro, Portugal and DFQ-UNIFEI, 37500-000 Itajubá, Brazil

N. A. Sobolev and M. A. Valente
Departamento de Física and I3N, Universidade de Aveiro, 3810-193 Aveiro, Portugal

K. Yamada
Institute for Materials Research, Tohoku University, 980-8577 Sendai, Japan

K. Sato
Institute of Symbiotic Science and Technology, TUAT, 184-8588 Tokyo, Japan

Y. Todate
Physics Department, Faculty of Science, Ochanomizu University, 2-1-1 Ohtsuka, Bunkyo-ku, Tokyo 112-8610, Japan

A. Bouravleuv
Institute of Symbiotic Science and Technology, TUAT, 184-8588 Tokyo, Japan and A.F. Ioffe Physico-Technical Institute, 194021 St. Petersburg, Russia

P. J. von Ranke
Instituto de Física, Universidade do Estado do Rio de Janeiro-UERJ, Rua Sao Francisco Xavier, 524, 20550-013, Rio de Janeiro, Brazil

S. Gama
Instituto de Física "Gleb Wataghin," Universidade Estadual de Campinas (UNICAMP), Caixa Postal 6165, Campinas 13, 083-970 São Paulo-SP, Brazil

(Received 8 November 2007; published 27 March 2008)

Manganese monophosphate MnP single crystal deserves attention due to its rich magnetic phase diagram, which is quite different depending on the direction of the applied magnetic field. Generally speaking, it has a Curie temperature around 291 K and several other magnetic arrangements at low temperatures (cone-, screw-, fan-, and ferromagnetic-type structures). This richness is due to the strong magnetocrystalline anisotropy. In this sense, the present paper makes a thorough description of the influence of this anisotropy on the magnetocaloric properties of this material. From a fundamental view we could point out, among those several magnetic arrangements, the most stable one. On the other hand, from an applied view, we could show that the magnetic entropy change around room temperature ranges from −4.7 to −3.2 J/kg K, when the magnetic field (5 T) is applied along the easy and hard magnetization directions, respectively. In addition, we have shown that it is also possible to take advantage of the magnetic anisotropy for magnetocaloric applications, i.e., we have found a quite flat magnetic entropy change (with a huge relative cooling power), at a fixed value of magnetic field, only rotating the crystal by 90°.

DOI: 10.1103/PhysRevB.77.104439 PACS number(s): 75.30.Sg, 75.30.Gw

I. INTRODUCTION

Magnetic refrigeration is a promising technology and therefore the attention of researchers to this subject is increasing in a fast pace. This technology, based on the magnetocaloric effect (discovered in 1881 by Warburg[1]), is of easy understanding: application of a magnetic field to a magnetic material, under adiabatic conditions, makes the temperature of such material to increase. On the other hand, under isothermal conditions (when the magnetic material is in thermal contact with a thermal reservoir), application of a magnetic field induces a heat exchange between the material and the reservoir. From these two processes it is possible to create a thermomagnetic cycle and thus a magnetocaloric device, such as air-conditioners, refrigerators, and more.

The physical quantities that measure the magnetocaloric potential are the magnetic entropy change ΔS and adiabatic temperature change ΔT. The magnetic entropy change is more common to be found in the literature, since we only need to know the magnetization map, i.e., $M(H,T)$, around the Curie temperature of the material. In addition to the quite

often use of the magnetic entropy change to characterize the magnetocaloric potential of materials, it is also used to understand the fundamental physical properties of the material.[2]

From the applied view, a lot of families of materials have been studied by the scientific community, which makes a great effort to find a good material for magnetocaloric application, i.e., a material of low cost, good thermal conductivity, low electrical resistivity, strong magnetocaloric effect (MCE), etc. We can cite some families: La-Fe-Si,[3,4] Gd-Si-Ge,[5–7] intermetallics,[8–11] and, mainly, the Mn-based materials, such as manganites,[2,12,13] shape memory alloys Ni_2MnGa,[14,15] MnFe(P,As),[16] and MnAs (Refs. 17–20) (it is also interesting to cite the 1950s pioneer work of Fakidov and Krasovskii[21] on the MCE of MnP polycrystal around room temperature). Concerning the MnAs compound, recently, some Brazilian groups published a series of papers presenting the colossal magnetic entropy change of this material.[17–20] At ambient pressure this material has 40 J/kg K at 318 K at 5 T, increasing up to 267 J/kg K at 280 K at 5 T at 2.2 kbar.[19] Small iron substitution on the Mn site, i.e., $Mn_{1-x}Fe_xAs$, induced a chemical pressure and therefore 320 J/kg K was obtained at 310 K, 5 T and ambient external pressure.[18] On the other hand, anisotropic magnetocaloric effect has also been extensively studied by several groups,[22–26] being a quite actual issue within the magnetocaloric research, since it fits applied and fundamental aspects.

In this sense, the MnP single crystal deserves attention due to two features: it belongs to the parent MnAs family and also has a strong magnetocrystalline anisotropy. Thus, the present paper has two branched ideas: from one side, we propose to take advantage of the strong magnetocrystalline anisotropy for magnetocaloric applications; and from the other side, we have used the magnetic entropy change to understand the fundamentals of the rich magnetic phase diagram that arises for this single crystal, also due to the magnetocrystalline anisotropy.

II. MnP PHASE DIAGRAM

MnP has an orthorhombic structure (a=5.92 Å, b=5.26 Å, c=3.17 Å),[27] belongs to the *Pnam* space group (62) and, in this paper, we define $a>b>c$. The phase diagram of MnP single crystal was already described in some papers.[27–32] The character of the magnetic phases, both in zero and nonzero magnetic fields, is influenced by the orthorhombic magnetocrystalline anisotropy. Below, we make a complete description of the phase diagram, drawn in Fig. 1, with the magnetic field applied to the three main directions of the crystal.

Magnetic field parallel to c axis (⟨001⟩)-easy axis. For low values of magnetic field, decreasing temperature, MnP becomes ferromagnetic (FM) at T_C=291 K, with its magnetic moment along this c (easy) axis. Further cooling leads to a first order transition at T_s=47 K, from FM to a screw (SCR) structure. In this SCR phase, the Mn magnetic moments are confined within the bc plane, perpendicular to the a axis. At 4 K a full rotation is completed roughly each 9a.[30]

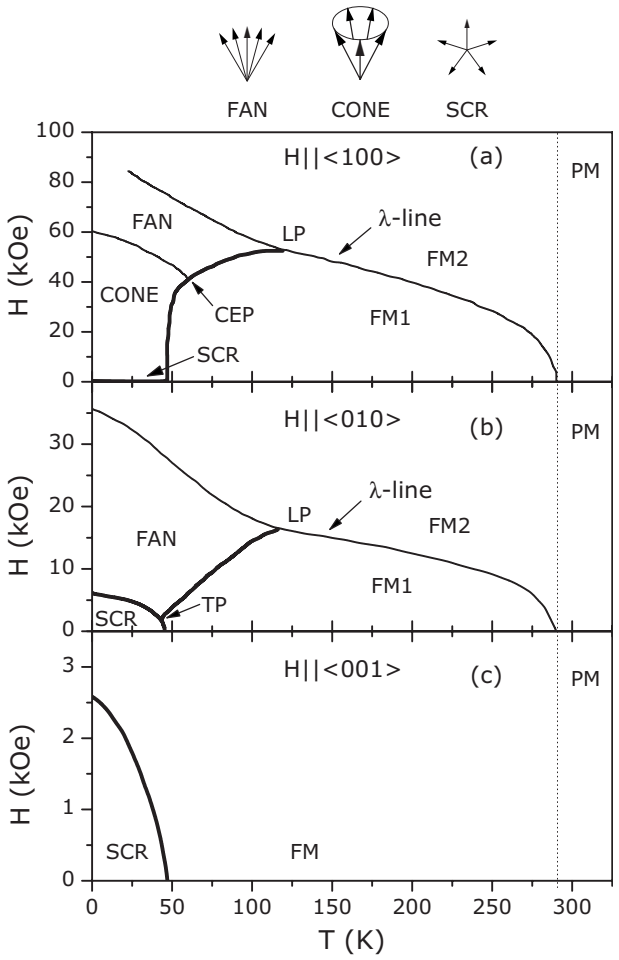

FIG. 1. Magnetic phase diagram of the MnP single crystal [after Zieba *et al.* (Ref. 32)]. These three panels correspond to the magnetic field applied along the three main directions of the crystal (⟨100⟩, ⟨010⟩, and ⟨001⟩). These labels have the following meaning: PM—paramagnetic phase, SCR—screw phase, FM1—magnetic moment along the ⟨001⟩ easy direction, FM2—magnetic moment along the applied magnetic field, CEP—critical end point, TP—triple point, and LP—Lifshitz point. The thick and thin lines represent, respectively, first and second order transitions.

At low temperatures (<47 K), increasing magnetic field, SCR phase changes back to the FM phase. This change in arrangement has a first order character. Figure 1(c) illustrates this phase diagram.

Magnetic field parallel to b axis (⟨010⟩)-intermediate axis. For low values of magnetic field, decreasing temperature, MnP also becomes ferromagnetic (FM1) at T_C=291 K, with its magnetic moment aligned along the c (easy) axis. Further cooling leads to a first order transition at T_s=47 K, from FM1 to the SCR structure. At low temperatures (<47 K), increasing magnetic field, SCR phase changes to FAN structure (first order transition). The difference with the SCR phase is that here (FAN), the magnetic moment does not perform a full rotation in the bc plane as we move along the a direction, but instead it oscillates about the b axis like a *fan*. Let us remember that in this case the magnetic field is applied along the ⟨010⟩ direction (b axis). Further increase of the magnetic field leads the system to a fully polarized ar-

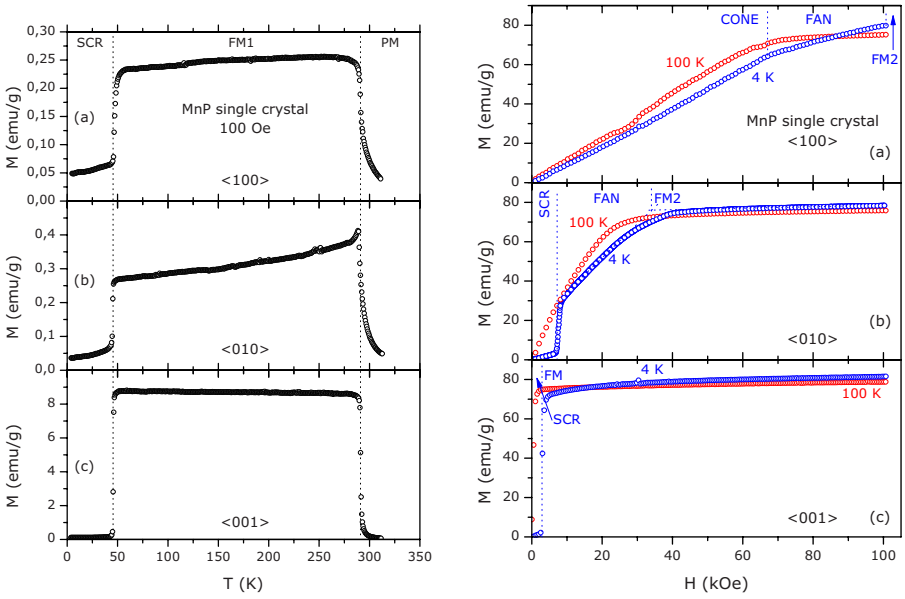

FIG. 2. (Color online) Magnetization as a function of temperature (left panels), and magnetic field (right panels). The magnetic field is applied along the three main crystallographic axes: (a) ⟨100⟩-hard, (b) ⟨010⟩-intermediate, and (c) ⟨001⟩-easy directions. See Sec. II and Fig. 1 for details concerning the labels.

rangement (FM2) along the b axis (second order transition). Between 47 K and the Lifshitz point (LP) at 121 K,[27,30,31] upon increasing the magnetic field, the system has a first order transition from the FM1 phase to the FAN phase and then to the FM2 phase. This line above which the magnetic moments are aligned along the magnetic field (i.e., FM2 phase) is called λ line.[27,30,31] For temperatures above LP it has a second order transition form the FM1 to FM2. To complete the description of this phase diagram, there is a triple point (TP), where the SCR, FAN, and FM1 phases merge. Figure 1(b) illustrates these transitions.

Magnetic field parallel to a axis (⟨100⟩)-hard axis. For low values of magnetic field, decreasing temperature, MnP also becomes ferromagnetic (FM1) at T_C=291 K, with its magnetic moment aligned along the c (easy) axis. Further cooling leads to a first order transition at T_s=47 K, from FM1 to the SCR structure. At low temperatures (<47 K), increasing magnetic field, SCR phase changes to a CONE phase, quite similar to the SCR phase; however, with a component along the a axis. Remember that, in this case, the magnetic field is applied along the ⟨100⟩ axis (a axis). Still increasing the magnetic field, the system changes to a FAN phase, oscillating about the a axis. Then, at high values of magnetic field, the system becomes fully polarized (FM2) along the a axis. This phase diagram is richer than the previous one (⟨010⟩ axis), and from 47 K up to the critical end point (CEP),[27,30,31] upon increasing magnetic field, the system has the same arrangements than before (<47 K); however, the ground state is FM1. Between CEP and LP the system changes from FM1 to FAN (first order transition) and then to FM2 (second order transition). For temperatures above LP, MnP has a second order transition, from FM1 to FM2. Details are given in Fig. 1(a).

III. EXPERIMENTAL DETAILS

Powders of manganese and phosphorus were sealed in an evacuated quartz double tube. The mixture was heated slowly (~40 °C/day) and kept 3 days at 900 °C. The reacted powder was melted at 1210 °C and the single crystal was grown by the Bridgman method at 1190 °C from this reaction product. The melting point of MnP is 1140 °C. The single crystal was further purified by the zone refining technique in a horizontal traveling furnace. The surface of the crystal was etched by nitric acid diluted with ethanol. The orientation of the crystal was determined by the x-ray Laue method. It has been confirmed by several neutron diffraction experiments that the mosaic spread of the crystal is quite small (less than 0.1°). Details of the sample preparation can be found in Ref. 33. Magnetization was measured in a vibrating sample magnetometer (VSM) magnetometer at the University of Aveiro, Portugal.

The sample is a cuboid with sides: a=1.50 mm, b=2.07 mm, and c=6.29 mm. The corresponding demagnetization factors (in SI units) are easy to obtain from Ref. 34: N_a=0.506, N_b=0.375, and N_c=0.119. From the results presented in this paper it is possible to estimate the demagnetization field. Let us consider, for instance, the highest demagnetization factor, i.e., that along the a axis. Thus, in this case, for 4 K and 10 T the demagnetization field is only 0.2 T and, consequently, the true magnetic field is 9.8 T.

IV. MAGNETIZATION MEASUREMENTS

As described before, our objective is to understand and describe the influence of the strong magnetocrystalline anisotropy on the magnetocaloric properties of MnP single crystal. We need to know the complete magnetization map, i.e., $M(T,H)$ to obtain the magnetic entropy change ΔS (a usual quantity to measure the magnetocaloric potential of materials), and it is done through the equation

$$\Delta S = \int_{H_i}^{H_f} \left(\frac{\partial M}{\partial T} \right)_H dH. \quad (1)$$

It is important to underline a minor point. The first order transitions present in this material have no hysteresis and

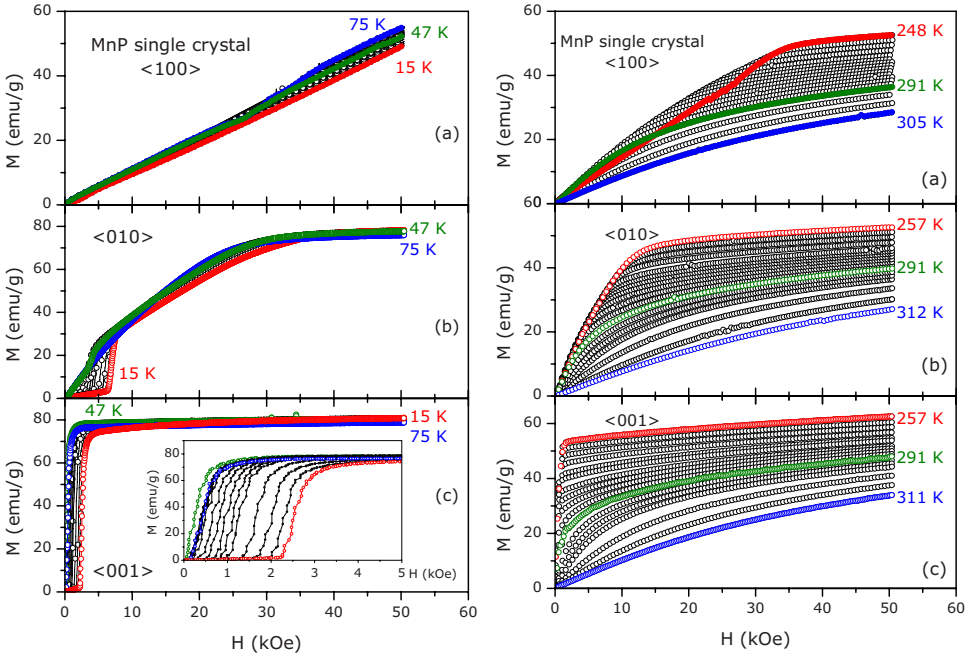

FIG. 3. (Color online) Magnetization as a function of magnetic field, applied along (a) ⟨100⟩, (b) ⟨010⟩, and (c) ⟨001⟩ directions. (left panels) These curves were taken at several temperatures around T_s=47 K, where the ground state changes from FM1 phase to SCR phase. (right panels) These curves were taken at several temperatures around T_c =291 K, where the ground state changes from PM phase to FM1 phase. See colored figures for clearness.

therefore we can consider that the equilibrium dynamics are faster than the measuring time. Thus, the system is in equilibrium and the Maxwell relation is valid.[35] When it is not the case, special care must be addressed.[36,37]

Thus, we first measured the magnetization as a function of temperature, with a low magnetic field (100 Oe), applied along the three main directions of the crystal: ⟨100⟩, ⟨010⟩, and ⟨001⟩. This result is presented in Fig. 2 (left panels) and shows two clear transitions, as described in the phase diagram (Sec. II). The first, at T_C=291 K, occurs from the paramagnetic phase (PM) to the ferromagnetic (FM1) phase, where the Mn moments are aligned along the *c*-easy axis, and the second transition, at T_s=47 K, occurs from the FM1 phase to the SCR phase. A minor point to clarify the labels: FM1 corresponds to the magnetic moment along ⟨001⟩ easy axis, whereas FM2 represents the magnetic moment along the applied field. Since these two cases are the same when $H \| \langle 001 \rangle$, we generally call this ferromagnetic phase as FM [see Fig. 1(c), for instance].

Figure 2 (right panels) is a clear example of the strong magnetocrystalline anisotropy in MnP single crystal and shows the magnetization as a function of magnetic field (up to 100 kOe) at 4 and 100 K, for those three crystallographic axes. We emphasize the agreement with the phase diagram described in Sec. II. The curves at 100 K do not have the phase changes as evident as those at 4 K.

As mentioned before, to obtain the magnetic entropy change we need to measure $M(T,H)$ around the magnetic transition. Thus, we measured those curves around T_s =47 K [Fig. 3 (left panels)] and T_C=291 K [Fig. 3 (right panels)], for those three main crystallographic axes. To clarify and confirm that phase diagram presented in Fig. 1, we show in Fig. 4 the magnetization as a function of temperature for several values of applied magnetic field, obtained by a treatment of those data of Fig. 3.

V. MAGNETIC ENTROPY CHANGE

From those data presented in the previous section and using Eq. (1) it is possible to determine the magnetic entropy change. Below we will discuss the behavior of this quantity when the magnetic field is applied along those three directions. The vertical dotted lines that appear in the figures of this section limit temperature ranges where there is a change in the magnetic arrangement due to the applied field. For instance, SCR→CONE means that the system, under a certain value of applied field, changed its magnetic arrangement from SCR to CONE phases.

A. Low temperature contribution

MCE of $H \| \langle 100 \rangle$: Around T_s=47 K there are five magnetic arrangements, namely, SCR, CONE, FAN, FM1, and FM2 (see Sec. II). Below 47 K we found a positive magnetic entropy change, where the system changes its arrangement from SCR to CONE [see Fig. 5(a)]. From this fact we can conclude that the SCR phase has a smaller magnetic entropy and is therefore more stable than the CONE phase. Around 47 K and for magnetic fields higher than 20 kOe there is a quite narrow range of temperatures where the FAN phase arises (between the CONE and FM1 phases—this behavior is a bit different than that presented in Fig. 1). See Fig. 4(a) for details. Due to the quite narrow temperature range, it is difficult to determine the magnetic arrangement from only magnetic measurements; however, the most probable arrangement, following the phase diagram of Fig. 1, is the FAN phase. We found therefore a deep minimum in the magnetic entropy curve [Fig. 5(a)—top]; in other words, a negative ΔS when the arrangement changes from SCR to FAN. This behavior is no more observed for $\Delta H < 20$ kOe [see Fig. 5(a)—bottom].

MCE of $H \| \langle 010 \rangle$: As described in Sec. II, increasing magnetic field, there are four magnetic arrangements around

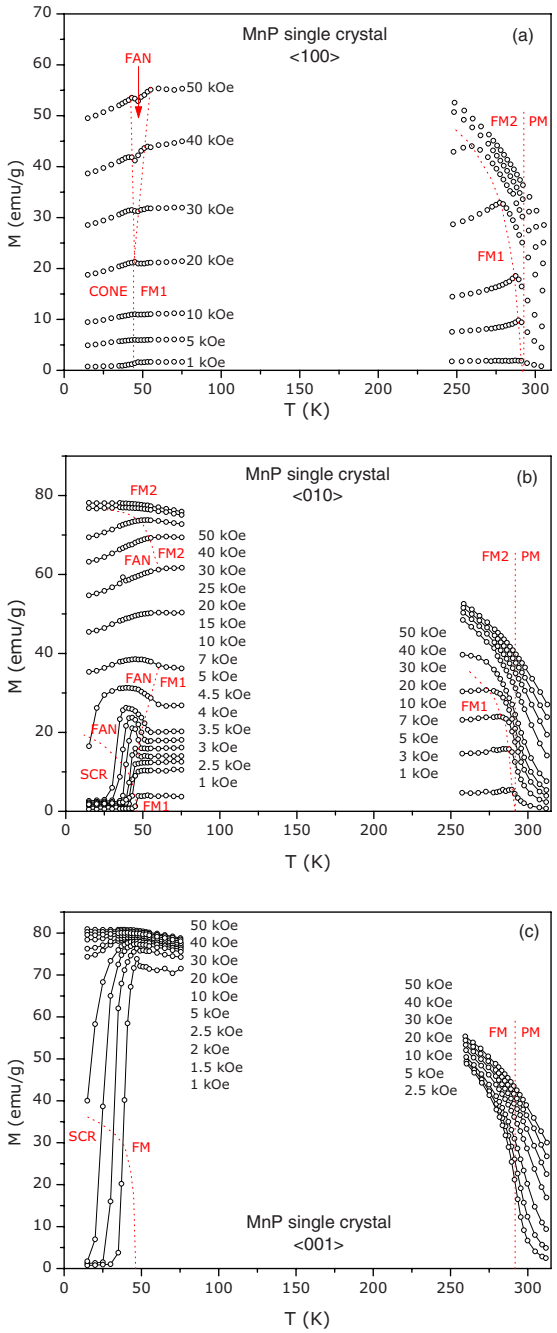

FIG. 4. (Color online) Magnetization as a function of temperature for several values of applied magnetic field along (a) ⟨100⟩, (b) ⟨010⟩, and (c) ⟨001⟩ directions. These curves were determined from Fig. 3. See Sec. II for the meaning of the labels.

T_s=47 K, namely, SCR, FAN, FM1, and FM2. Below 47 K, we found a positive magnetic entropy change when the system changes its arrangement from SCR to FM2 and FAN phases [see Fig. 5(b)]. We conclude from this fact that the SCR phase has a magnetic entropy smaller than the FM2 and FAN phases and, consequently, is more stable. This fact is confirmed by the zero magnetic entropy change for magnetic field changes within the SCR phase [$\Delta H \lesssim 5$ kOe, namely, 5 kOe (blue curve) and 1 kOe (red curve) see Fig. 5(b)—bottom]; i.e., this phase is stable enough that those values of magnetic field are not able to change the entropy of that phase (SCR).

A different scenario arises above 47 K, where the magnetic entropy change is negative. Here, the magnetic entropy of the FM1 phase is bigger than the FM2 and FAN phases; and is, consequently, less stable than the FM2 and FAN arrangements. Figure 5(b)—top clarifies the above discussion, for magnetic field change from zero up to above the λ line. Figure 5(b)—bottom also sketches those words, however, for intermediate values of magnetic field change.

MCE of $H\|\langle 001\rangle$: In a similar fashion as described before, for temperatures below 47 K the magnetic entropy change is positive, indicating that the SCR phase is more stable than the FM phase. We remember that in this case FM=FM1=FM2, since the magnetic moment is aligned along the ⟨001⟩ directions (FM1) and also along the magnetic field (FM2); thus, we generally call this phase as FM. Again, the magnetic field change within the SCR phase is not able to change the entropy of this phase and, consequently, the corresponding magnetic entropy change is zero. Above 47 K, the magnetic entropy change becomes negative, indicating, in this case with only one arrangement above 47 K (FM), the usual behavior of increasing entropy by decreasing magnetic field. Details are sketched in Fig. 5(c).

B. High temperature contribution

MCE of $H\|\langle 100\rangle$: As shown in Fig. 6, the magnetic entropy change above the Curie temperature T_C=291 K, i.e., in the paramagnetic phase, is negative, as expected. Below T_C in a limited temperature range (from FM1 to FM2), the magnetic entropy change is also negative; and shows that the FM1 phase has a bigger magnetic entropy than the FM2 phase. Thus, FM2 is more stable than the FM1 phase.

On the other hand, the magnetic entropy change becomes positive when the magnetic field change is not enough to cross the λ line, i.e., the arrangement does not change and remains within the FM1 phase. It means that magnetic entropy of the FM1 phase under applied magnetic field (below the λ line) is bigger than the magnetic entropy with a lower value of magnetic field (or even a zero magnetic field). Consequently, we conclude that the FM1 phase without magnetic field is more stable than the same phase with applied magnetic field (below the λ line). This conclusion is reasonable, because the strong magnetocrystalline anisotropy tends to align the magnetic moment along ⟨001⟩ direction (FM1), and this situation has a lower entropy than the "perturbed" case where the spins are submitted to a magnetic field (below the λ line) along the ⟨100⟩ direction. Figure 6(a) clarifies this scenario. Note that these positive values agree with the same measurement at low temperatures [see Fig. 5(a)].

MCE of $H\|\langle 010\rangle$: In a similar fashion as before, the magnetic entropy change (a) within the paramagnetic phase and (b) between the FM1 and FM2 phases are both negatives, as expected. In addition, the magnetic entropy change is (almost) zero changing the arrangement within the FM1 phase. It means that applying the magnetic field (below the λ line) along the ⟨010⟩ direction does not change the entropy of the system (different from the ⟨100⟩ case, where the entropy evi-

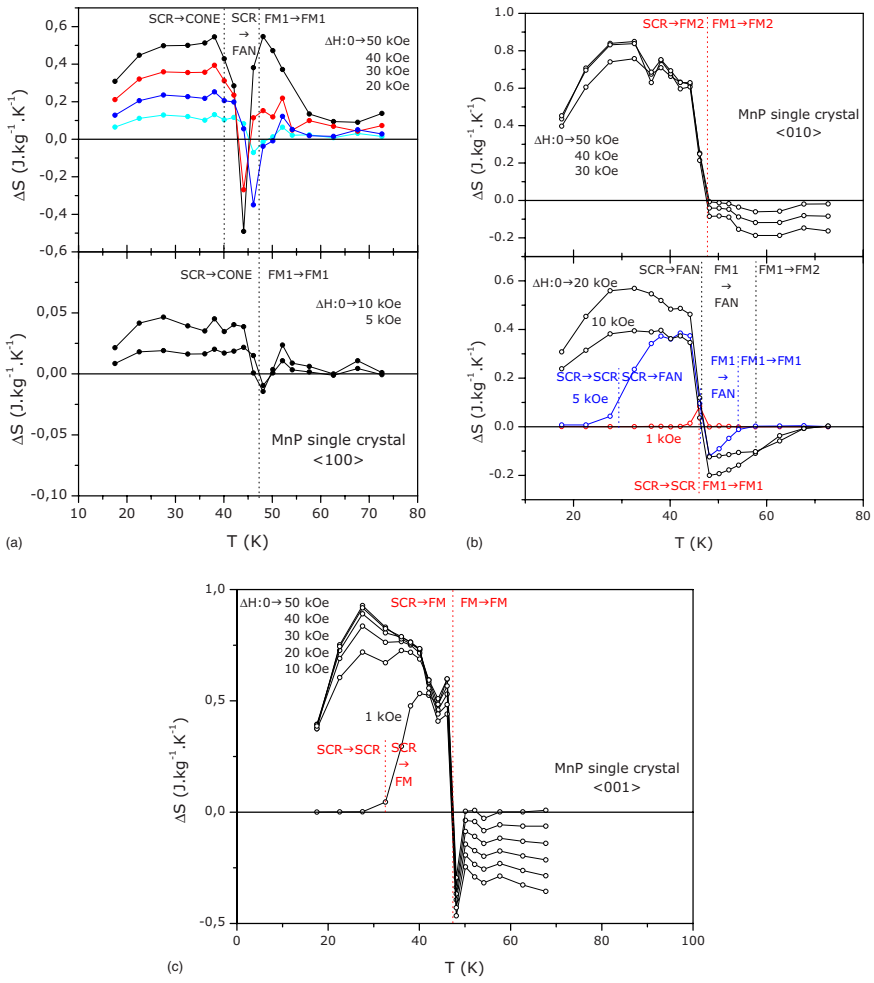

FIG. 5. (Color online) Magnetic entropy change as a function of temperature (around T_s=47 K), when the magnetic field is applied along the (a) ⟨100⟩, (b) ⟨010⟩, and (c) ⟨001⟩ directions. The vertical dotted lines limit temperature ranges where the magnetic arrangement changes due to the applied field. See colored figures for clearness.

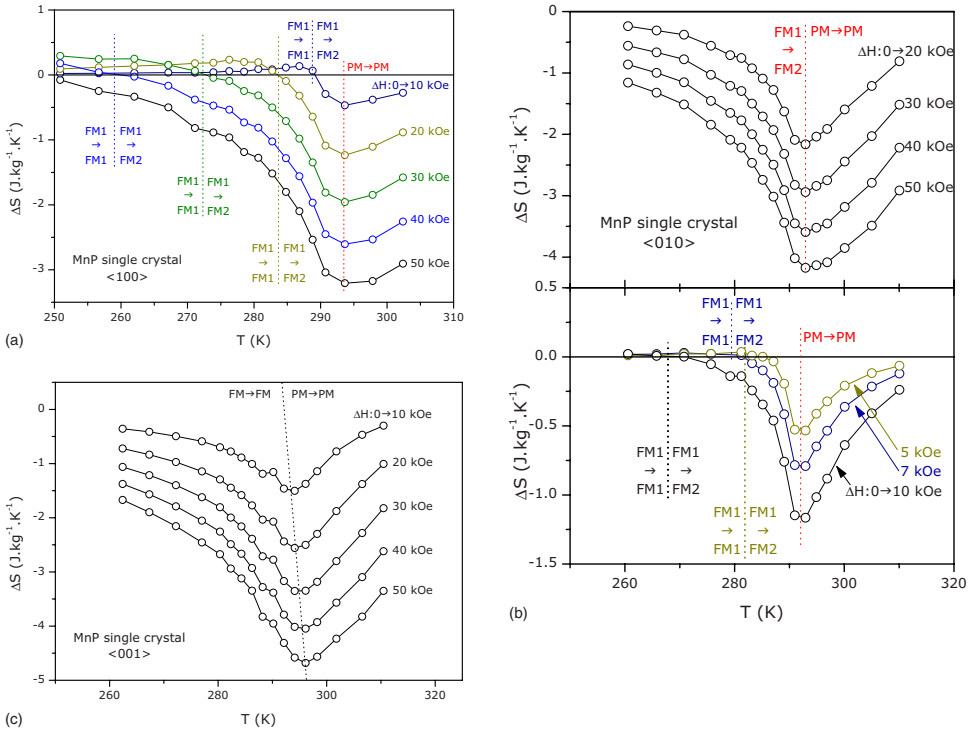

FIG. 6. (Color online) Magnetic entropy change as a function of temperature (around T_C =291 K), when the magnetic field is applied along the (a) ⟨100⟩, (b) ⟨010⟩, and (c) ⟨001⟩ directions. The vertical dotted lines limit temperature ranges where the magnetic arrangement changes due to the applied field. See colored figures for clearness/

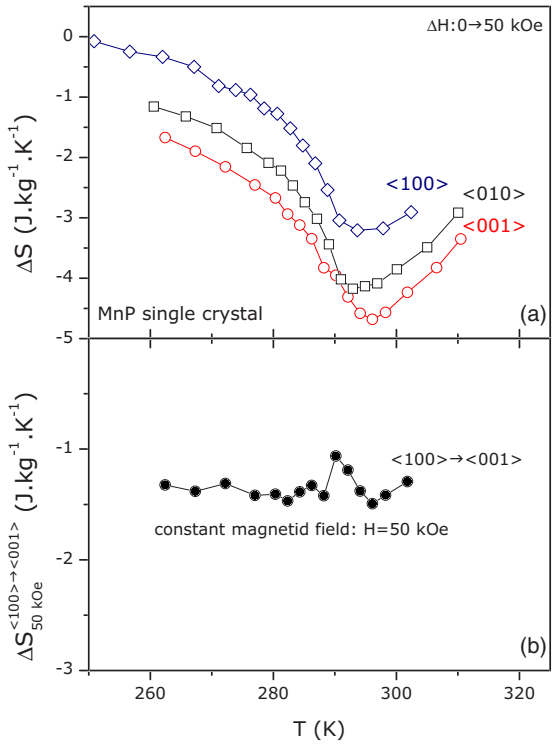

FIG. 7. (Color online) (a) Magnetic entropy change for 50 kOe of magnetic field change applied along the three main crystallographic axes ⟨100⟩, ⟨010⟩, and ⟨001⟩. This difference is therefore due to the strong magnetic anisotropy present in this MnP single crystal. (b) Magnetic entropy change for a fixed magnetic field (50 kOe), just rotating the crystal, from the hard (⟨100⟩) to the easy (⟨001⟩) direction. In other words, it is the magnetic entropy change due to the anisotropy.

dently increases). See Fig. 6(b) for clearness.

MCE of $H\|\langle 001\rangle$: It is the simplest case and has a usual magnetic entropy change curve, without changes in the magnetic arrangement by changing the magnetic field. Figure 6(c) presents these results.

VI. ADVANTAGES OF THE MAGNETOCRYSTALLINE ANISOTROPY FOR MAGNETOCALORIC APPLICATIONS

In this section we analyze the advantages of the magnetic anisotropy for magnetocaloric applications around the Curie temperature (T_C=291 K), which is close to room temperature (RT). It is expected, due to the anisotropy, that the magnetic entropy change measured with the magnetic field applied along the hard direction be smaller than that along the easy direction, and indeed it is [see Fig. 7(a)]. We can note that there is 1.5 J/kg K (at 50 kOe) of entropy change between those curves (around T_C) and this energy can be achieved only rotating the crystal, from the hard to the easy direction under a fixed value of magnetic field. The magnetic entropy change due to this rotation is equal to the difference of entropy change due to the applied field along those hard and easy directions as follows:

$$\Delta S_{50\ \mathrm{kOe}}^{\langle 100\rangle\rightarrow\langle 001\rangle} = \Delta S^{\langle 001\rangle} - \Delta S^{\langle 100\rangle} = S_{50\ \mathrm{kOe}}^{\langle 001\rangle} - S_{0\ \mathrm{kOe}}^{\langle 001\rangle} - (S_{50\ \mathrm{kOe}}^{\langle 100\rangle} - S_{0\ \mathrm{kOe}}^{\langle 100\rangle}) = S_{50\ \mathrm{kOe}}^{\langle 001\rangle} - S_{50\ \mathrm{kOe}}^{\langle 100\rangle}. \quad (2)$$

Considering, of course, that the zero field entropy is isotropic, i.e., $S_{0\ \mathrm{kOe}}^{\langle 001\rangle}=S_{0\ \mathrm{kOe}}^{\langle 001\rangle}=S_{0\ \mathrm{kOe}}$. Figure 7(b) presents therefore $\Delta S_{50\ \mathrm{kOe}}^{\langle 100\rangle\rightarrow\langle 001\rangle}$. We should emphasize the quite flat profile of the magnetic entropy change upon rotating the crystal. In spite of low absolute value of magnetic entropy change, it has a giant relative cooling power[38] due to the huge width at half maximum.

VII. FINAL REMARKS

The present paper has two branched ideas: from one side, we used the magnetic entropy change to understand the rich phase diagram of MnP single crystal, with several magnetic arrangements due to the strong magnetocrystalline anisotropy. We could discuss therefore which magnetic phase is more stable. From the other side, after Refs. 24 and 25, we could generally propose how to take advantage of the anisotropy for magnetocaloric applications: we could obtain a quite flat magnetic entropy change around the Curie temperature of the system (~291 K) at a constant magnetic field, only rotating the crystal. This flat ΔS is an advantage of the anisotropy, since a magnetic refrigerator based on this idea does not need to move permanent magnets, but only rotate a single crystal refrigerant material by 90° under a constant magnetic field.

ACKNOWLEDGMENT

M.S.R. thanks FCT for the project POCI/CTM/61284/2004. The authors thank (i) FCT for the VSM equipment (REEQ/1126/2001) and (ii) Sérgio Pereira for the orientation of the sample. R.M.R. also thanks FCT for the grant (SFRH/BPD/34541/2007).

*marior@ua.pt

[1] E. Warburg, Ann. Phys. **13**, 141 (1881).
[2] M. S. Reis, V. S. Amaral, J. P. Araújo, P. B. Tavares, A. M. Gomes, and I. S. Oliveira, Phys. Rev. B **71**, 144413 (2005).
[3] A. Fujita, S. Fujieda, Y. Hasegawa, and K. Fukamichi, Phys. Rev. B **67**, 104416 (2003).
[4] A. Fujita, S. Fujieda, K. Fukamichi, H. Mitamura, and T. Goto, Phys. Rev. B **65**, 014410 (2001).
[5] V. K. Pecharsky and K. A. Gschneidner, Jr., Phys. Rev. Lett. **78**, 4494 (1997).
[6] W. Choe, V. K. Pecharsky, A. O. Pecharsky, K. A. Gschneidner, V. G. Young, and G. J. Miller, Phys. Rev. Lett. **84**, 4617 (2000).
[7] V. K. Pecharsky, A. P. Holm, K. A. Gschneidner, and R. Rink, Phys. Rev. Lett. **91**, 197204 (2003).

[8] D. Wang, H. Liu, S. Tang, S. Yang, S. Huang, and Y. Du, Phys. Lett. A **297**, 247 (2002).
[9] N. A. de Oliveira, P. J. von Ranke, and A. Troper, Phys. Rev. B **69**, 064421 (2004).
[10] P. J. von Ranke, E. P. Nóbrega, I. G. de Oliveira, A. M. Gomes, and R. S. Sarthour, Phys. Rev. B **63**, 184406 (2001).
[11] A. Gomes, M. Reis, I. Oliveira, A. Guimaraes, and A. Takeuchi, J. Magn. Magn. Mater. **242**, 870 (2002).
[12] D. Morelli, A. Mance, J. Mantese, and A. Micheli, J. Appl. Phys. **79**, 373 (1996).
[13] H. Chen, C. Lin, and D. Dai, J. Magn. Magn. Mater. **257**, 254 (2003).
[14] F. Xia Hu, B. Gen Shen, and J. Rong Sun, Appl. Phys. Lett. **76**, 3460 (2000).
[15] X. Zhou, W. Li, H. Kunkel, and G. Williams, J. Phys.: Condens. Matter **16**, L39 (2004).
[16] O. Tegus, E. Brück, L. Zhang, Dagula, K. Buschow, and F. de-Boer, Physica B **319**, 174 (2002).
[17] D. Rocco, A. Campos, A. Carvalho, L. Caron, P. von Ranke, and N. Oliveira, Appl. Phys. Lett. **90**, 242507 (2007).
[18] A. Campos, D. Rocco, A. Carvalho, L. Caron, A. Coelho, S. Gama, L. Silva, F. Gandra, A. Santos, L. Cardoso, P. J. Von Ranke, and N. A. Oliveira, Nat. Mater. **5**, 802 (2006).
[19] S. Gama, A. A. Coelho, A. de Campos, A. M. Carvalho, F. C. G. Gandra, P. J. von Ranke, and N. A. de Oliveira, Phys. Rev. Lett. **93**, 237202 (2004).
[20] P. J. von Ranke, S. Gama, A. A. Coelho, A. Campos, A. M. Carvalho, F. C. G. Gandra, and N. A. de Oliveira, Phys. Rev. B **73**, 014415 (2006).
[21] I. Fakidov and V. Krasovskii, Sov. Phys. JETP **9**, 755 (1959).
[22] M. Mihalik and V. Sechovsky, J. Magn. Magn. Mater. **310**, 1758 (2007).
[23] P. von Ranke, N. Oliveira, V. Sousa, D. Garcia, I. Oliveira, A. Carvalho, and S. Gama, J. Magn. Magn. Mater. **313**, 176 (2007).
[24] P. von Ranke, N. Oliveira, C. Mello, D. Garcia, V. Sousa, V. Souza, A. Caldas, and I. Oliveira, J. Alloys Compd. **440**, 46 (2007).
[25] M. Zou, Y. Mudryk, V. K. Pecharsky, K. A. Gschneidner, D. L. Schlagel, and T. A. Lograsso, Phys. Rev. B **75**, 024418 (2007).
[26] P. J. von Ranke, N. A. de Oliveira, D. C. Garcia, V. S. R. de Sousa, V. A. de Souza, A. M. Carvalho, S. Gama, and M. S. Reis, Phys. Rev. B **75**, 184420 (2007).
[27] C. C. Becerra, V. Bindilatti, and N. F. Oliveira, Phys. Rev. B **62**, 8965 (2000).
[28] E. E. Huber and D. H. Ridgley, Phys. Rev. **135**, A1033 (1964).
[29] T. Komatsubara, H. Shinohara, T. Suzuki, and E. Hirahara, J. Appl. Phys. **40**, 1037 (1969).
[30] C. C. Becerra, H. J. Brumatto, and N. F. Oliveira, Phys. Rev. B **54**, 15997 (1996).
[31] Y. Shapira, C. C. Becerra, N. F. Oliveira, and T. S. Chang, Phys. Rev. B **24**, 2780 (1981).
[32] A. Zieba, C. C. Becerra, H. Fjellvag, N. F. Oliveira, and A. Kjekshus, Phys. Rev. B **46**, 3380 (1992).
[33] Y. Todate, K. Yamada, Y. Endoh, and Y. Ishikawa, J. Phys. Soc. Jpn. **56**, 36 (1987).
[34] A. Aharoni, J. Appl. Phys. **83**, 3432 (1998).
[35] J. S. Amaral (private communication).
[36] A. Tishin and Y. Spichkin, *The Magnetocaloric Effect and its Applications* (Institute of Physics, Bristol, 2003).
[37] K. Gschneidner, V. Pecharskyand, and A. Tsokol, Rep. Prog. Phys. **68**, 1479 (2005).
[38] The relative cooling power is defined as the maximum value of the magnetic entropy change curve (i.e., ΔS_{max}) times the width of this curve at half maximum.